

# Partial Differential Equation-based GPR Signature Discrimination for Automatic Detection of Bridge Deck Delamination

Zhe Wendy Wang, *Student Member IEEE*, Greg Slabaugh, *Member IEEE* and Tong Fang, *Member IEEE*

**Abstract**—Accurate assessment of the quality of concrete bridge decks and identification of corrosion induced delamination leads to economic management of bridge decks. It has been demonstrated that ground penetrating radar (GPR) can be successfully used for such purposes. The growing demand on GPR has brought into the challenge of developing automatic processes necessary to produce a final accurate interpretation. However, there have been few publications targeting at automatic detection of bridge deck delamination from GPR data. This paper proposes a novel method using partial differential equations (PDEs) to detect rebar (or steel-bar) mat signatures of concrete bridges from GPR data so that the delamination within the bridge deck can be effectively located. The proposed algorithm was tested on both synthetic and real GPR data and the experimental results have demonstrated its accuracy and reliability, even for diminished contrast and low signal-to-noise ratio.

**Index Terms**—Partial Differential Equations, Ground Penetrating Radar, Automatic Detection, Image Processing

## I. INTRODUCTION

The I-35 highway bridge collapsed into the Mississippi river during rush hour on August 1, 2007. Approximately 100 vehicles were involved and thirteen deaths were attributed to the collapse. This tragedy signifies that the condition of the bridges in the United States is deteriorating and requires enormous financial and human resources for its maintenance and mitigation. An important component of the inspection and rehabilitation of concrete bridges is the assessment of the bridge deck condition. The advent of nondestructive evaluation techniques has significantly aided this task, and several methods have been successfully utilized to detect common defects in concrete bridge decks. Among these methods, Ground Penetrating Radar (GPR) is one of the most widely used techniques nowadays.

While it is capable of detecting deck delaminations at various stages of deterioration, precise interpretation of the measured parameters has yet to be fully automated. The post-processing procedures leading to the final interpretation still suffer from some drawbacks, such as excessive reliance on experienced operators' intervention and scan-by-scan processing. Significant improvements to the automation of a bridge condition evaluation process are expected to come from imaging and image processing techniques.

On the GPR record, potential areas of deterioration appear as zones of attenuation. Delamination is most likely to occur

around rebar mats within the concrete. Typically, corroded rebar has a lower dielectric constant than good iron or steel, producing a weaker reflection on the radar record. Therefore, the amplitude of reflection and attenuation are measured as an indication of delamination of the rebar mat from the concrete and deterioration of the concrete. Our work is targeting at the automatic detection of bridge deck delamination.

A crucial component of automatic bridge condition evaluation is the detection of corroded rebars, as delamination always occurs around rebars. Due to the GPR imaging principle, the reflected wave feature of the rebar mat is a series of hyperbolas and the top of each hyperbola denotes the corresponding rebar's position. Despite its importance, however, no literature can be found about hyperbolas series specific fitting algorithm for GPR data from bridge deck.

Cylindrical objects such as buried pipes appear in the GPR scans as hyperbolas. There have been several hyperbolic signature detection methods in literature for the applications such as detection of distinct landmine or buried pipe. Among these methods, migration is a commonly used frequency domain method and it collapses hyperbolas into short linear regions [1]. Another trend is using neural network or fuzzy logic to detect arc signatures in GPR scans [2]–[6]. However, none of these methods is devised for the corroded rebar mats in concrete bridges, which is much more difficult to detect than the ordinary buried utilities. Most GPR-related data processing work tends to rely on less sophisticated techniques for hyperbolic signature detection, and thus suffers from drawbacks caused by noise, such as the detector in [7], being only able to detect good and good-minus signatures, which is not suitable for delamination detection.

In this paper, we for the first time propose a novel method based on partial differential equations (PDEs) to discriminate rebar mat signatures for bridge deck delamination detection in GPR scans. We first detect the apex of each rebar using a template-based method with a similarity metric of sum of squared difference (SSD) and then estimate the parameters of each hyperbola in the GPR scans with a PDE method.

The rest of this paper is organized as follows. Section II describes the characteristic shape of rebar signature. Section III proposes a novel PDE-based detection method. Section IV provides results that demonstrate the ability of the proposed method to detect rebar signatures in GPR scans, even for images of diminished contrast and low signal-to-noise ratio.

Z. W. Wang is with the Department of Electrical and Computer Engineering, New Jersey Institute of Technology, Newark, NJ, 07102 USA [zw27@njit.edu](mailto:zw27@njit.edu)

G. Slabaugh and T. Fang are with Intelligent Vision and Reasoning Department, Siemens Corporate Research, Princeton, NJ 08540, USA. [greg.slabaugh](mailto:greg.slabaugh), [tong.fang@siemens.com](mailto:tong.fang@siemens.com)

## II. HYPERBOLIC SIGNATURES

Locating rebar mat is usually done by noting hyperbolic shapes in the GPR image, as indicated in Fig. 1 (Color printout is needed for better readability for all figures). A series of hyperbolas are shown in the GPR image, with some of the hyperbolic signatures being blurred. The apex of each hyperbola locates each rebar. These hyperbolas occur due to the reason that the antenna transmits energy in a conical pattern. Consequently, it receives reflections from the rebar at decreasing two-way travel time as it approaches the rebar, then increasing the travel time after passing over the rebar. Areas of the rebar mat exhibiting weak reflection amplitude are typically indicative of deterioration.

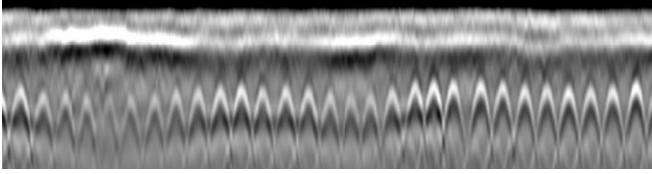


Fig. 1. Rebar Signature in a GPR image.

Let a point  $\mathbf{p}$  in a south-opening hyperbola be expressed as

$$\mathbf{p} = \begin{bmatrix} x \\ y \end{bmatrix} = \begin{bmatrix} x \\ a\sqrt{1 + (x-h)^2/b^2} + k \end{bmatrix} \quad (1)$$

where  $(x,y)$  is the coordinate,  $(h,k)$  is the center point,  $a$  and  $b$  are the shape parameters. The asymptotes cross at the center of the hyperbola and have slope  $\pm \frac{a}{b}$  for the south-opening hyperbola. The hyperbola profile is depicted in Fig. 2.

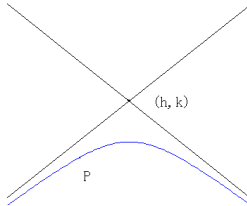


Fig. 2. Hyperbola profile

It is worth noting that there are four degrees of freedom for the hyperbola profile fitting according to Eq. (1) while some researchers use the equation modelling the hyperbolic signatures from GPR data in the form as follows [7][8],

$$\frac{y^2}{a^2} - \frac{(x-h)^2}{b^2} = 1 \quad (2)$$

Only three degrees of freedom are employed in the above equation for the hyperbola fitting. Moreover, it is based on the assumption that the modelled signatures result from point reflectors, which cannot be guaranteed in the case of rebar mat.

## III. SIGNATURE DISCRIMINATION BASED ON PDE

The proposed scheme consists of two major stages: first, using a template based method, we detect the apex of the hyperbolic signatures. Next, we fit the hyperbola curves to the GPR image data using partial differential equations in an iterative fashion, with the initial guess of the center point modified from the apex obtained in the previous step.

### A. SSD Based Hyperbola Center Point Detection

In this step, we use a template, as shown in the box in Fig. 3, to match the rebar signature based on the similarity metric of sum of squared difference (SSD), defined as follows.

$$SSD = \sum_x \sum_y (T(x,y) - I_w(x,y))^2 \quad (3)$$

where  $T(x,y)$  and  $I_w(x,y)$  denote the template image and the region over a sliding window in the GPR image, respectively. When these two images are geometrically aligned, the SSD value reaches its minimum. SSD is chosen as it offers sufficient accuracy and is simple to implement.

We first search the minimum SSD values along each column in the whole GPR image and the one that contributes to minimum SSD values is selected as a reference rebar apex position. Since the interval between two adjacent rebars is usually fixed, we then exploit the periodicity of the hyperbolic signatures so as to detect all the rebars. To determine the periodicity, Fast Fourier Transform (FFT) is applied. Therefore, with the assistance of reference rebar and periodicity of hyperbolic signatures, apex positions of all the rebars are obtained. Afterwards, the knowledge is incorporated to the PDEs as the initial guess of center point of each hyperbola for the next step.

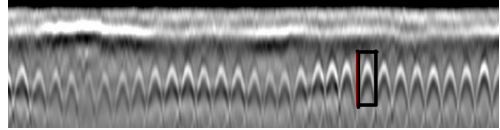


Fig. 3. A template in a GPR image.

### B. Hyperbolic Signature Discrimination

Our goal is to fit the hyperbola curve  $l$  to the GPR image data. To accomplish this, an energy function is designed as

$$E = \int_{l_1}^{l_2} I(\mathbf{p}) dl \quad (4)$$

where  $I(\mathbf{p})$  is the intensity of pixel  $\mathbf{p}$  and the integral is along the hyperbola from point  $p_1$  to  $p_2$ . By maximizing this energy function, the intensity of the image data along the hyperbola achieves its maximum. Therefore, the hyperbola curve is fit to the GPR scan.

Starting with an initial guess, we can iteratively update the hyperbola parameters using PDEs to maximize the energy function in Eq. (4). Note that, we use the position of the hyperbola center point obtained from the previous step as the initial guess of  $h$  and  $k$ .

Using a chain rule, differentiation of energy function  $E$  with respect to parameter  $a$  gives

$$\frac{\partial E}{\partial a} = \int_I \nabla I \cdot \frac{\partial \mathbf{p}}{\partial a} dl \quad (5)$$

where  $\nabla I$  is the gradient of the image,  $\frac{\partial \mathbf{p}}{\partial a} = \begin{bmatrix} 0 \\ \frac{\partial y}{\partial a} \end{bmatrix}$

We solve  $\frac{\partial y}{\partial a}$  according to Eq. (1) as

$$\frac{\partial y}{\partial a} = \sqrt{1 + (x-h)^2/b^2} \quad (6)$$

In a similar fashion, we can calculate the expressions for  $\frac{\partial \mathbf{p}}{\partial b}$ ,  $\frac{\partial \mathbf{p}}{\partial h}$  and  $\frac{\partial \mathbf{p}}{\partial k}$ . Clearly,  $\frac{\partial x}{\partial b} = \frac{\partial x}{\partial h} = \frac{\partial x}{\partial k} = 0$ . Next, we derive  $\frac{\partial y}{\partial b}$ ,  $\frac{\partial y}{\partial h}$  and  $\frac{\partial y}{\partial k}$ .

Differentiation of  $y$  with respect to  $b$ ,  $h$  and  $k$ , can be expressed respectively as

$$\begin{aligned} \frac{\partial y}{\partial b} &= a \cdot \frac{1}{2} \cdot \frac{1}{\sqrt{1 + (x-h)^2/b^2}} \cdot (-2) \cdot (x-h)^2 \cdot \frac{1}{b^3} \\ &= -\frac{a(x-h)^2}{b^3 \sqrt{1 + (x-h)^2/b^2}} \end{aligned} \quad (7)$$

$$\begin{aligned} \frac{\partial y}{\partial h} &= a \cdot \frac{1}{2} \cdot \frac{1}{\sqrt{1 + (x-h)^2/b^2}} \cdot \left(\frac{-1}{b^2}\right) \cdot 2(x-h) \\ &= -\frac{a(x-h)}{b^2 \sqrt{1 + (x-h)^2/b^2}} \end{aligned} \quad (8)$$

$$\frac{\partial y}{\partial k} = 1 \quad (9)$$

In order to maximize the energy function, we use a gradient ascent method, *i.e.*,

$$\mathbf{r}_{n+1} = \mathbf{r}_n - \gamma \cdot \nabla E(\mathbf{r}_n) \quad (10)$$

where  $\mathbf{r}_n = \begin{bmatrix} a_n \\ b_n \\ h_n \\ k_n \end{bmatrix}$  and  $\gamma$  is the step-size parameter. Eq. (10)

is iterated until the maximum number of iteration step is reached or the prescribed accuracy is met, *i.e.*,  $\|\mathbf{r}_{n+1} - \mathbf{r}_n\| \leq \varepsilon$ , where  $\varepsilon$  is a given small positive value.

#### IV. EXPERIMENTAL RESULTS

In the experiments, we begin with synthetically generated data, designed to study the detection performance as the contrast level is diminished, as depicted in Fig. 4. To quantify the detection performance with respect to the diminishing contrast, which occurs around corroded rebars, we calculate the distance between the ground truth and the detected hyperbolas as the detection error, defined as follows.

$$D = \frac{1}{n} \sqrt{\sum_i^n d_i^2} \quad (11)$$

where  $n$  is the number of pixels along the rebar curves and  $d_i$  is the Euclidean distance between the  $i$ th point in the original hyperbola and the corresponding point in the detected curve. From Fig. 5, we can observe that the detection performance does not degrade when the contrast is diminished.

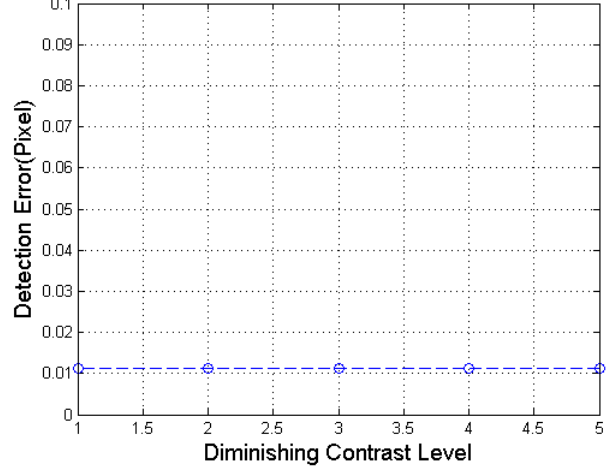


Fig. 5. Detection Error as a function of diminishing contrast.

To evaluate the algorithm performance with respect to signal-to-noise ratio (SNR), we devise another set of experiments, as depicted in Fig. 6. Similarly, we calculate the distance between the ground truth and the detected hyperbolas as the detection error, according to Eq. (11). From Fig. 7, it is obvious to notice that the proposed method is very robust to decreasing SNR or increasing noise level.

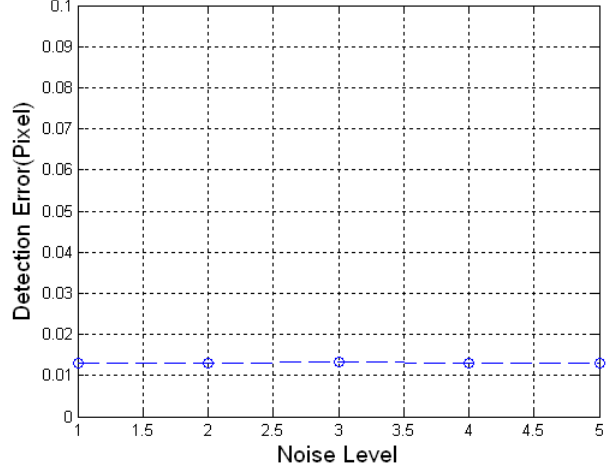


Fig. 7. Detection Error as a function of decreased SNR.

We also examine the effectiveness of the proposed scheme for real GPR scans of bridges, as depicted in Fig. 8(a) and Fig. 9(a). The pulse transmitted by GPR is usually displayed in an image as a characteristic dark-light-dark series of bands. The results are fairly clear. Our method detects the bright rebar hyperbolic signatures accurately, even in the attenuation zones where the rebar has less contrast.

#### V. CONCLUSIONS

The tragedy of I-35 bridge collapse still lingers in people's minds. Nobody is willing to see that history repeats itself.

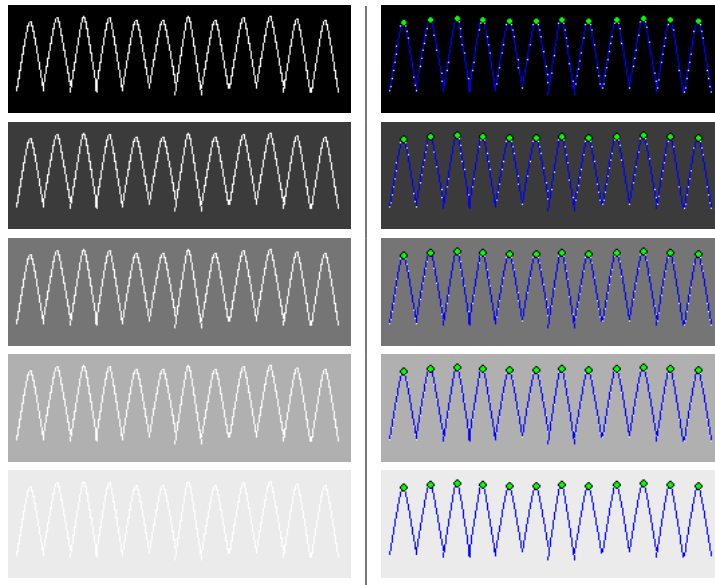


Fig. 4. Rebar detection in synthetic GPR images. The left column shows the original synthetic GPR Images with contrast level being diminished. The right column is the detection results.

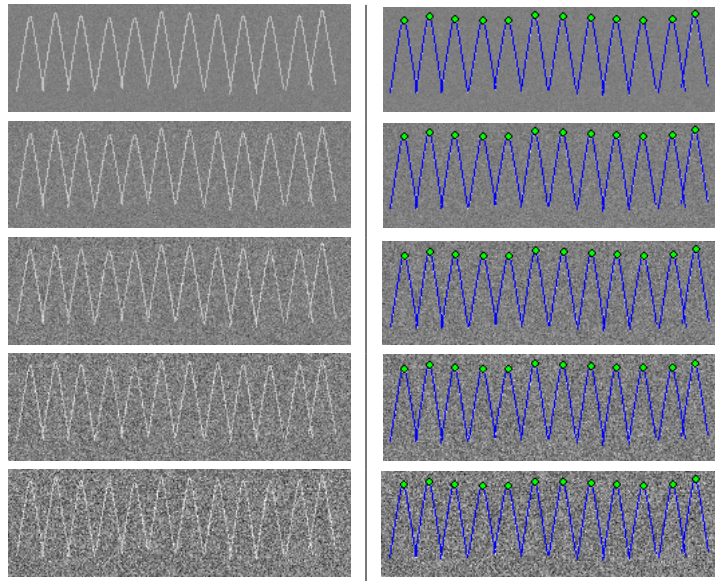


Fig. 6. Rebar detection in synthetic GPR images. The left column is the original synthetic GPR Images with SNR being decreased. The right column is the detection results.

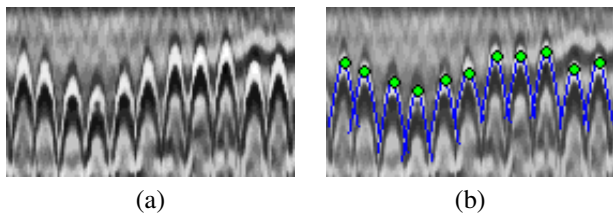


Fig. 9. Rebar detection in a GPR image. (a) Original GPR Image, and (b) Rebar detection result.

to detect the rebar mat of bridge deck in GPR scans. Our experiments have demonstrated the ability of this method to accurately detect rebars in GPR scans, even for diminishing contrast and low SNR. The results presented in the paper indicate that the proposed method has much promise in automatic delamination detection of bridge decks.

Therefore, accurate bridge deck assessment is of significant importance. This paper proposes a novel method using PDEs

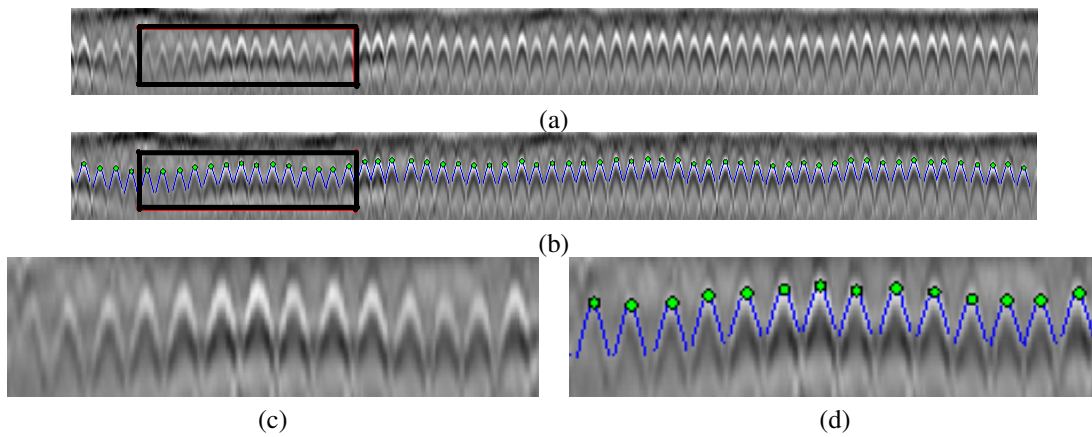


Fig. 8. Rebar detection in a GPR image. (a) Original GPR image , (b) Rebar detection result , (c) Highlighted and enlarged region in the original GPR image, and (d) Highlighted and enlarged region in detection result.

#### REFERENCES

- [1] D. Huston, P. Fuhr, K. Maser, and W. Weedon, "Nondestructive testing of reinforced concrete bridges using radar imaging techniques," *Final Research Report NETC 94-2 for New England Transportation Consortium*, February 2000.
- [2] S. Delbo, P. Gamba, and D. Roccatto, "A fuzzy shell clustering approach to recognize hyperbolic signatures in subsurface radar images," *IEEE Trans. Geosci. Remote Sensing*, vol. 38, no. 3, May 2000.
- [3] P. Gamba and S. Lossani, "Neural detection of pipe signatures in ground penetrating radar images," *IEEE Trans. Geosci. Remote Sensing*, vol. 38, no. 2, March 2000.
- [4] P. D. Gader, J. M. Keller, and B. N. Nelson, "Recognition technology for the detection of buried landmines," *IEEE Trans. Fuzzy Syst.*, vol. 9, no. 1, Feb. 2001.
- [5] P. D. Gader, B. N. Nelson, H. Frigui, G. Vailllette, and J. M. Keller, "Fuzzy logic detection of landmines with ground penetrating radar," *Signal Process.*, vol. 80, no. 6, 2000.
- [6] W. Al-Nuaimy, Y. Huang, M. Nakhkash, M. T. C. Fang, V. T. Nguyen, and A. Eriksen, "Automatic detection of buried utilities and solid objects with gpr using neural networks and pattern recognition," *Journal of Applied Geophysics*, vol. 43, no. 2-4, 2000.
- [7] V. Krause, I. Abdel-Qader, O. Abudayyeh, and S. Yehia, "An image segmentation algorithm for the detection of rebar in bridge decks from gpr scans," in *Proc. IEEE International Conference on Electro/Information Technology*, Chicago, U.S., May 2007, pp. 114 – 119.